

# Negative-parity states of odd Xe and Ba isotopes in the interacting boson-fermion model

S. T. Hsieh and H. C. Chiang\*

*Department of Physics, National Tsing Hua University, Hsinchu, Taiwan 30043, Republic of China*

M. M. King Yen

*Department of Nuclear Engineering, National Tsing Hua University, Hsinchu, Taiwan 30043, Republic of China*

(Received 19 December 1989)

The negative-parity states of odd xenon and odd barium isotopes have been interpreted within the framework of the interacting boson-fermion model where the multi-orbit boson-fermion interaction is simplified. Comparisons with observed energy spectra as well as other model calculations are made.

The odd-mass, transitional nuclides  $^{117-131}\text{Xe}$  and  $^{123-133}\text{Ba}$  have been analyzed within the framework of the interacting boson-fermion model I (IBFA-1).<sup>1</sup> The xenon isotopes have also been studied using IBFA-2, distinguishing neutrons from protons.<sup>2</sup> In both works, the single  $j$ -orbit formalism is generalized to the multilevel situation through the BCS occupation number correlation factors appearing in the boson-fermion interactions. However, such an approach may be too restrictive in that it overemphasized the pairing interaction.<sup>3</sup> Furthermore, it was suggested that the correlation effect may even be absorbed in the renormalizations of the single  $j$ -orbit boson-fermion interaction parameters.<sup>4</sup> This makes things much simpler. Actual calculations in this spirit were carried out for the positive-parity states in those odd-mass xenon isotopes and barium isotopes.<sup>5</sup> With just two boson-fermion interaction parameters systematically varying from isotope to isotope, all quasibands are reasonably reproduced, as well as known  $B(E2)$  values of xenon. Therefore, the relaxation of the BCS correlations of the boson-fermion interactions seems to be justified.

The experimental data for the negative-parity states go to even higher values both in spin and in excitation energy, providing another test. We apply the same method to the negative-parity states in this work.

The basis states in IBFA-1 consist of single fermion states coupled to boson core states. Three single-particle orbits ( $1h_{11/2}$ ,  $1h_{9/2}$ , and  $2f_{7/2}$ ) are allowed for the fermion to move in and IBA-1 basis states are used for the boson core.

The model Hamiltonian has three parts. For the boson part, a four-term Hamiltonian is usually adequate:

$$H_B = \epsilon_d n_d + a_0 P^\dagger \cdot P + a_1 L \cdot L + a_2 Q \cdot Q.$$

The fermion part is just the quasiparticle energy term:

$$H_F = \sum_{j,m} \epsilon_j a_{jm}^\dagger a_{jm}.$$

Finally, the boson-fermion part can be simply represented by the quadrupole and the exchange interactions:

$$H_{BF} = K[(s^\dagger \times \tilde{d} + d^\dagger \times \tilde{s})^{(2)} - \frac{\sqrt{7}}{2}(d^\dagger \times \tilde{d})^{(2)}] \sum_{j_1, j_2} \frac{1}{\sqrt{5}} \langle j_1 \| Y^{(2)} \| j_2 \rangle (a_{j_1}^\dagger \times \tilde{a}_{j_2})^{(2)} \\ - 2\Lambda \sum_{j_1, j_2, k} \left[ \frac{5}{2k+1} \right]^{1/2} \langle j_1 \| Y^{(2)} \| k \rangle \langle k \| Y^{(2)} \| j_2 \rangle : [(a_{j_1}^\dagger \times \tilde{d})^{(k)} \times (d^\dagger \times \tilde{a}_{j_2})^{(k)}]^{(0)} :,$$

TABLE I. Top part: Relevant even xenon cores with boson number  $N$  (explained in the text) and  $d$ -boson energy  $\epsilon_d$  (in MeV). The other parameters  $a_0$ ,  $a_1$ , and  $a_2$  are plotted in Fig. 1. Bottom part: Interaction parameters for odd xenon isotopes.

|                     | $^{116}\text{Xe}$ | $^{118}\text{Xe}$ | $^{122}\text{Xe}$ | $^{124}\text{Xe}$ | $^{126}\text{Xe}$ | $^{128}\text{Xe}$ | $^{130}\text{Xe}$ | $^{132}\text{Xe}$ |
|---------------------|-------------------|-------------------|-------------------|-------------------|-------------------|-------------------|-------------------|-------------------|
| $N$                 | 8                 | 9                 | 9                 | 8                 | 7                 | 6                 | 5                 | 4                 |
| $\epsilon_d$        | 0.65              | 0.60              | 0.62              | 0.63              | 0.64              | 0.69              | 0.78              | 0.86              |
|                     | $^{117}\text{Xe}$ | $^{119}\text{Xe}$ | $^{121}\text{Xe}$ | $^{123}\text{Xe}$ | $^{125}\text{Xe}$ | $^{127}\text{Xe}$ | $^{129}\text{Xe}$ | $^{131}\text{Xe}$ |
| $\Delta\epsilon_d$  | 0.4266            | 0.5189            | 0.2451            | 0.2063            | 0.2063            | 0.1472            | 0.0715            | 0.0576            |
| $K$                 | -0.05             | -0.05             | -0.04             | -0.04             | -0.04             | -0.04             | -0.04             | -0.04             |
| $\Lambda$           | -1.2063           | -1.3099           | -0.5666           | -0.5504           | -0.5460           | -0.4433           | -0.2812           | -0.2812           |
| $\epsilon(h_{9/2})$ | -0.5468           | -0.7769           | -0.3800           | -0.3800           | -0.3131           | -0.1628           | *                 | 0.0867            |
| $\epsilon(f_{7/2})$ | 0.054             | 0.064             | 0.031             | 0.039             | *                 | *                 | *                 | *                 |

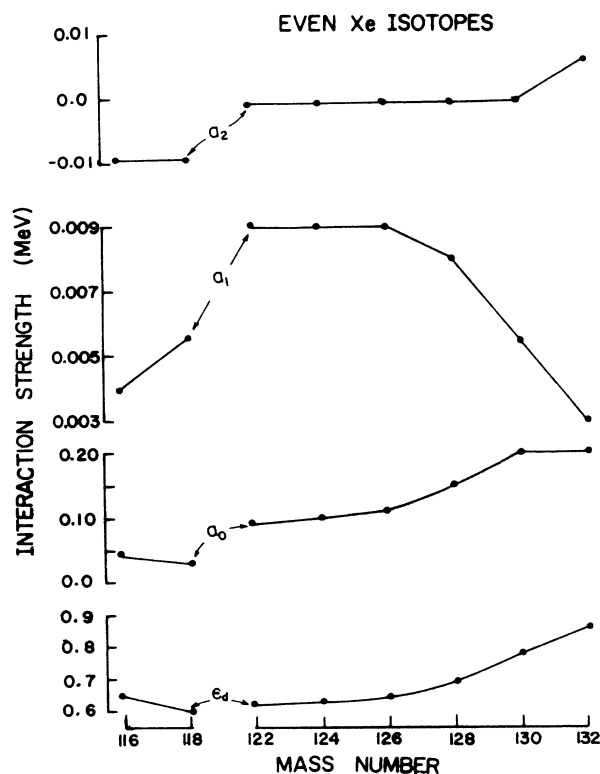


FIG. 1. Variation of boson interaction parameters for even xenon isotopes.

with the understanding that (1) the effect of the monopole term will be absorbed in  $\epsilon_d$  through a "renormalization" of  $\epsilon_d$ ; (2) the BCS occupation number correlation factors are neglected. The plausibility and justification have been given in the above.

To fix the interaction parameters  $\epsilon_d$ ,  $a_0$ ,  $a_1$ , and  $a_2$  of the boson Hamiltonian, a least-squares fit on the energy spectra of the even core nuclei is performed first. The results are either listed on the upper part of Tables I and II or plotted in Fig. 1. The boson number  $N$  is obtained taking  $Z=50, N=82$  as the inert core, except for  $^{116}\text{Xe}$  and  $^{118}\text{Xe}$  nuclei where  $N=50$  is used instead. As examples,  $^{117}\text{Xe}$  is viewed as an eight boson plus one fermion system whereas  $^{121}\text{Xe}$  is a nine boson (in which seven of them are boson holes) plus one fermion (also a hole) system. Therefore, the parameters behave smoothly from  $^{132}\text{Xe}$  to  $^{122}\text{Xe}$  but not necessarily to  $^{118}\text{Xe}$  as can be seen in Fig. 1. The quality of the least-squares fit is shown in Fig. 2, taking  $^{118}\text{Xe}$  as an example.

Going to the odd-mass isotopes,  $\epsilon_d$  is expected to change in order to absorb the effect of the monopole interaction which has been left out. In addition, we have the quadrupole strength  $K$ , the exchange parameter  $\Lambda$ , and quasiparticle energies  $\epsilon(h_{9/2})$  and  $\epsilon(f_{7/2})$  [assuming  $\epsilon(h_{11/2})=0$ ] to fit the various energy spectra.

The resulting  $d$ -boson energy  $\epsilon_d$  was found to increase quite a bit with respect to those of the even core. The values  $\Delta\epsilon_d$  listed in the middle row of Tables I and II

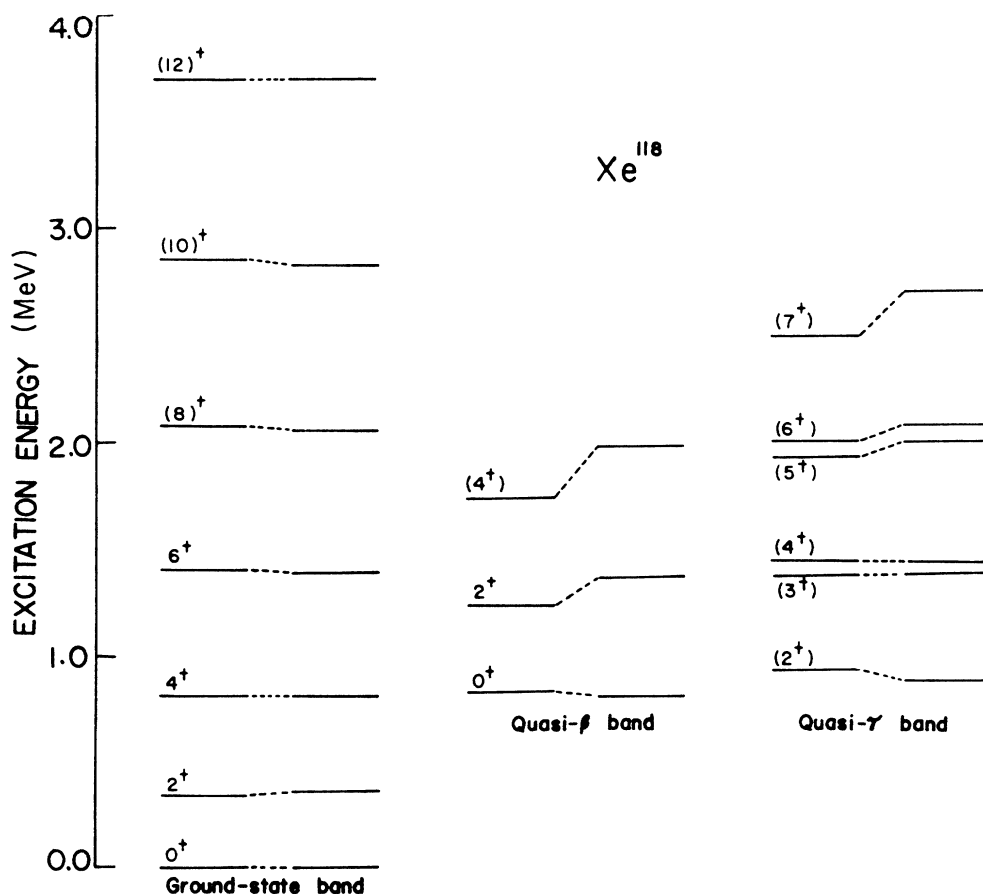


FIG. 2. The experimental and the calculated energy spectra for  $^{118}\text{Xe}$ . Observed levels from Ref. 7 are plotted on the left column with  $J^\pi$  assignment while the calculated ones are on the right.

TABLE II. Interaction parameters for barium isotopes. See caption for Table I.

|                     | <sup>124</sup> Ba | <sup>126</sup> Ba | <sup>128</sup> Ba | <sup>130</sup> Ba | <sup>132</sup> Ba | <sup>134</sup> Ba |
|---------------------|-------------------|-------------------|-------------------|-------------------|-------------------|-------------------|
| $N$                 | 10                | 9                 | 8                 | 7                 | 6                 | 5                 |
| $\epsilon_d$        | 0.66              | 0.66              | 0.66              | 0.66              | 0.68              | 0.76              |
|                     | <sup>123</sup> Ba | <sup>125</sup> Ba | <sup>127</sup> Ba | <sup>129</sup> Ba | <sup>131</sup> Ba | <sup>133</sup> Ba |
| $\Delta\epsilon_d$  | 0.1836            | 0.1429            | 0.1429            | 0.1110            | 0.                | -0.0461           |
| $K$                 | -0.023            | -0.023            | -0.023            | -0.023            | -0.023            | -0.0433           |
| $\Lambda$           | -0.2039           | -0.2039           | -0.1151           | -0.0993           | 0.1324            | 0.4063            |
| $\epsilon(h_{9/2})$ | -0.2855           | -0.1556           | -0.1186           | -0.0816           | -0.0767           | *                 |
| $\epsilon(f_{7/2})$ | -0.4823           | -0.3761           | *                 | *                 | *                 | *                 |

TABLE III. Calculated wave function intensities associated with the configurations of each fermion single-particle orbit for <sup>123</sup>Xe and <sup>123</sup>Ba.

| <sup>123</sup> Xe | $\frac{7}{2}^-$ | $\frac{9}{2}^-$ | $\frac{11}{2}^-$ | $(\frac{13}{2})_1^-$ | $(\frac{13}{2})_2^-$ | $(\frac{15}{2})_1^-$ | $(\frac{15}{2})_2^-$ | $(\frac{15}{2})_3^-$ | $\frac{17}{2}^-$ | $\frac{19}{2}^-$ | $\frac{21}{2}^-$ | $\frac{23}{2}^-$ |
|-------------------|-----------------|-----------------|------------------|----------------------|----------------------|----------------------|----------------------|----------------------|------------------|------------------|------------------|------------------|
| $h_{11/2}$        | 0.095           | 0.002           | 0.816            | 0.836                | 0.026                | 0.847                | 0.332                | 0.394                | 0.823            | 0.883            | 0.845            | 0.913            |
| $h_{9/2}$         | 0.003           | 0.984           | 0.003            | 0.038                | 0.926                | 0.002                | 0.522                | 0.307                | 0.039            | 0.001            | 0.032            | 0.001            |
| $f_{7/2}$         | 0.902           | 0.015           | 0.182            | 0.126                | 0.047                | 0.152                | 0.146                | 0.300                | 0.138            | 0.116            | 0.123            | 0.086            |
| <sup>123</sup> Ba | $\frac{7}{2}^-$ | $\frac{9}{2}^-$ | $\frac{11}{2}^-$ | $\frac{13}{2}^-$     | $\frac{15}{2}^-$     | $\frac{17}{2}^-$     | $\frac{19}{2}^-$     | $\frac{21}{2}^-$     | $\frac{23}{2}^-$ | $\frac{25}{2}^-$ | $\frac{27}{2}^-$ |                  |
| $h_{11/2}$        | 0.013           | 0.004           | 0.814            | 0.723                | 0.865                | 0.765                | 0.926                | 0.803                | 0.965            | 0.833            | 0.981            |                  |
| $h_{9/2}$         | 0.008           | 0.895           | 0.075            | 0.235                | 0.057                | 0.216                | 0.046                | 0.186                | 0.027            | 0.106            | 0.016            |                  |
| $f_{7/2}$         | 0.979           | 0.100           | 0.110            | 0.042                | 0.078                | 0.019                | 0.028                | 0.011                | 0.008            | 0.007            | 0.003            |                  |

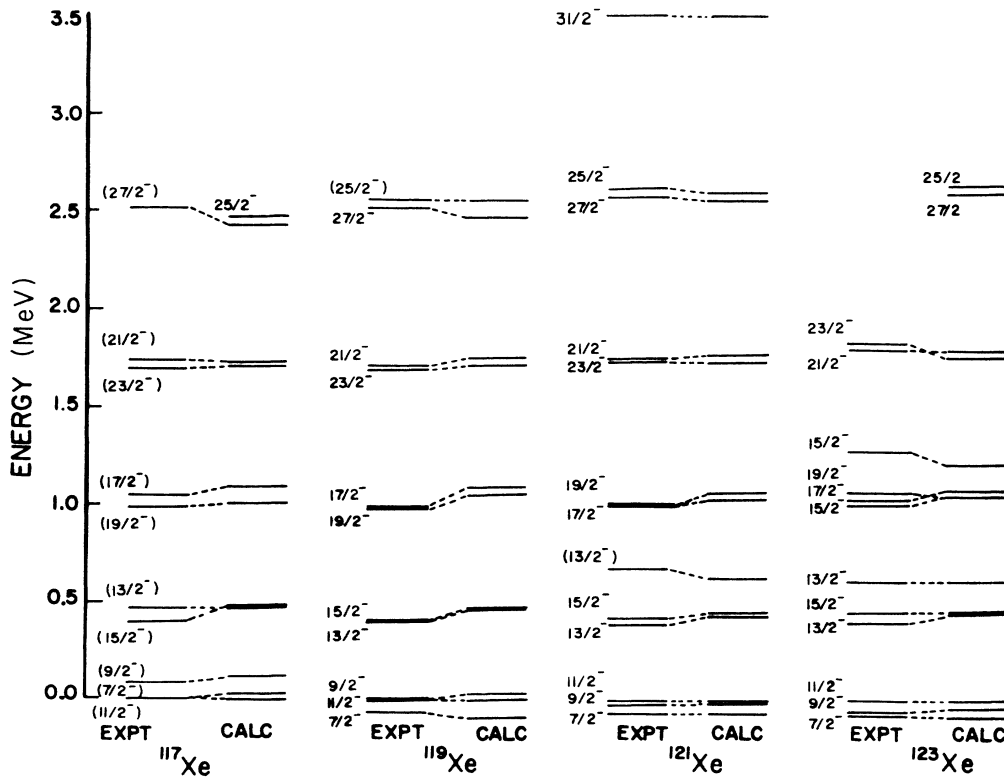


FIG. 3. The experimental and the calculated energy spectra for Xe-117, -119, -121, and -123. The experimental data are taken from Refs. 8–10.

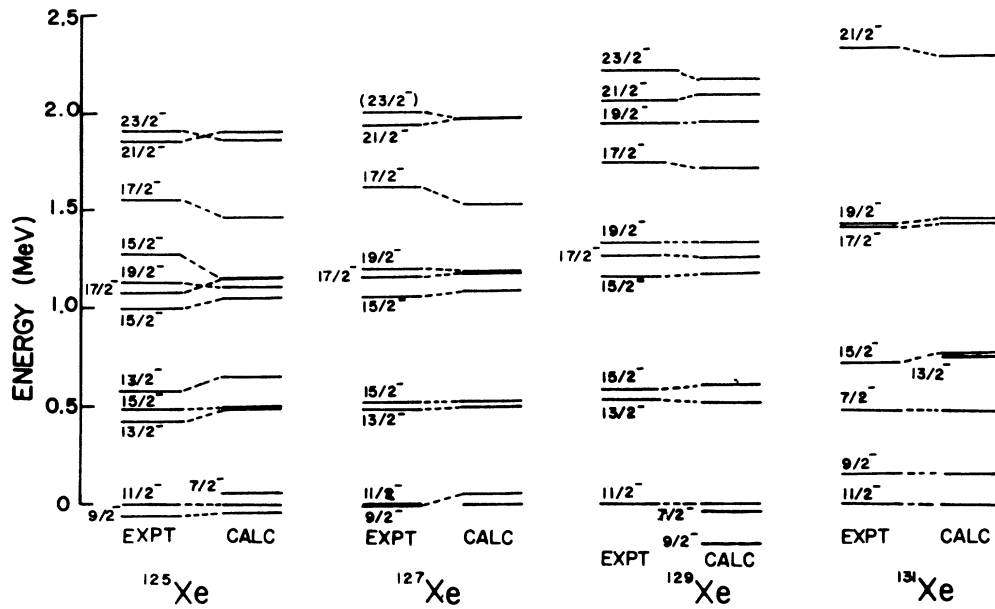


FIG. 4. The experimental and the calculated energy spectra for Xe-125, -127, -129, and -131. The experimental data are taken from Refs. 11–13.

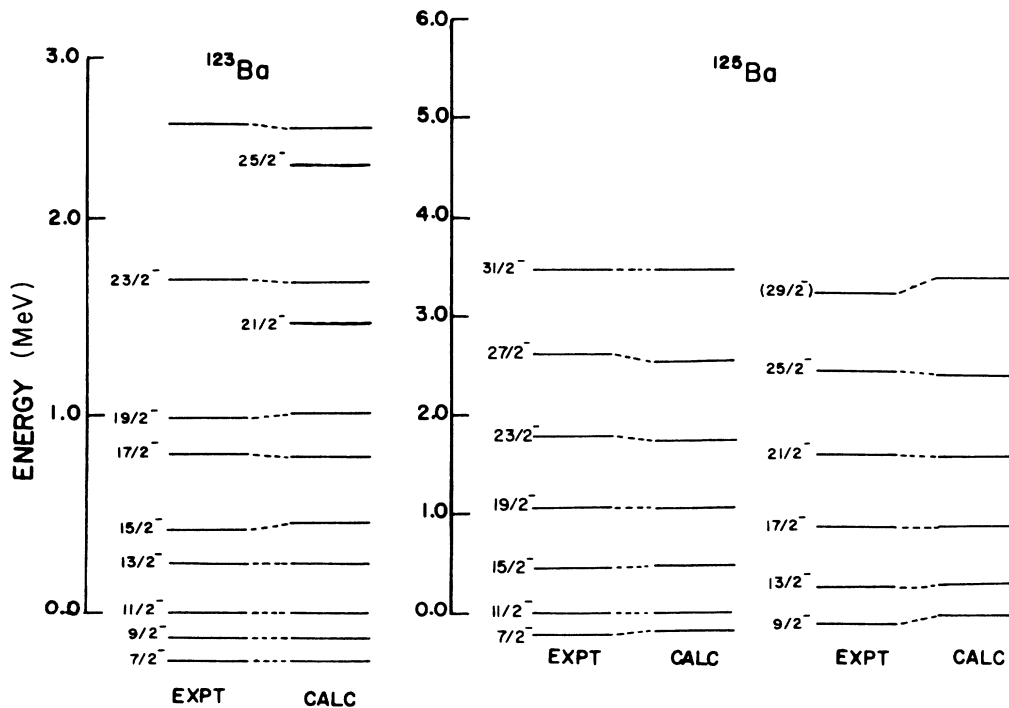


FIG. 5. The experimental and the calculated energy spectra for Ba-123 and -125. The data are taken from Refs. 14, 15, and 16.

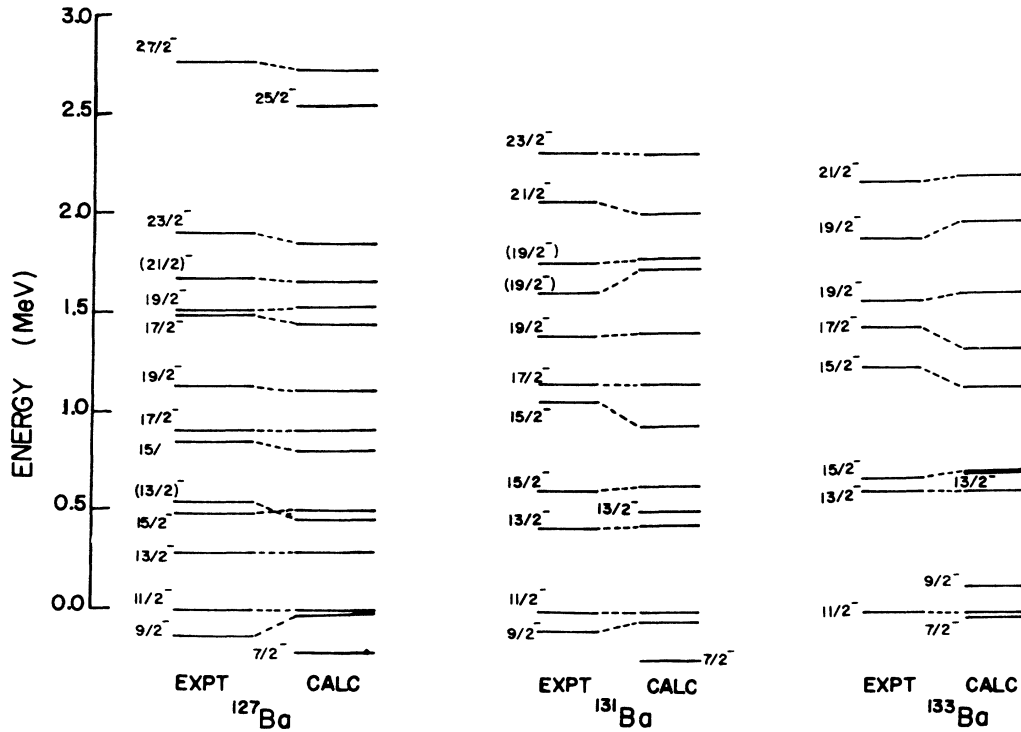


FIG. 6. The experimental and the calculated energy spectra for Ba-127, -131, and -133. The data are taken from Refs. 17, 15, and 19.

represent that increase. This indicates that the renormalization brought up by the monopole term is not negligible, an aspect rather different from the positive-parity results.<sup>5</sup> The effect decreases as the boson number goes down. For  $^{133}\text{Ba}$ ,  $\Delta\epsilon_d$  turns negative. The quadrupole

parameter  $K$  can almost be kept constant within each isotope series except for  $^{133}\text{Ba}$ , which has the smallest boson number. Using the quasiparticle energies calculated from BCS,<sup>1</sup> the exchange strength  $\Lambda$  alone cannot reproduce both the  $\frac{9}{2}^-$  and  $\frac{7}{2}^-$  energy levels as well as the narrow gaps between the  $\frac{13}{2}^-$ - $\frac{15}{2}^-$  pair and the  $\frac{17}{2}^-$ - $\frac{19}{2}^-$  pair. Therefore  $\epsilon(h_{9/2})$  and  $\epsilon(f_{7/2})$  were varied freely to fit the spectra. Resulting parameters are listed in the bottom part of Tables I and II. For some nuclides, the  $\frac{7}{2}^-$  or  $\frac{9}{2}^-$  level is not yet observed. Naturally we cannot be very sure of the corresponding quasiparticle energy. Those cases are indicated by asterisks in the tables. Unfortunately, due to differences in the models, it is difficult to compare our interaction parameters with those of other works.

The energy spectra calculated using the above interaction parameters are compared with the observed data. Figures 3 and 4 show results for the xenon isotopes. The energies are relative to the  $\frac{11}{2}^-$  level. General features and narrow gaps are quite well reproduced. Inevitably there are certain inversions of states at some narrow gaps. The largest deviations occur for the first  $\frac{5}{2}^-$  state in  $^{117}\text{Xe}$  and the second  $\frac{23}{2}^-$  state in  $^{129}\text{Xe}$ . Apparently these states cannot be explained with our model and are omitted in the figures. The calculation also predicts more narrow gaps: a  $\frac{25}{2}^-$  level just above the  $\frac{27}{2}^-$  level of  $^{117}\text{Xe}$ ; a  $\frac{29}{2}^-$  level just above the  $\frac{31}{2}^-$  level and a  $\frac{33}{2}^-$  level above the  $\frac{35}{2}^-$  level in  $^{121}\text{Xe}$  (not shown in the figure), a  $\frac{25}{2}^-$  level above the  $\frac{27}{2}^-$  in  $^{123}\text{Xe}$ ; and a  $\frac{13}{2}^-$  level just below the  $\frac{15}{2}^-$  level of  $^{131}\text{Xe}$ . However, the calculated positions of the yet unobserved  $\frac{7}{2}^-$  (and also  $\frac{9}{2}^-$  in  $^{127}\text{Xe}$ ) states in Xe-125, -127, and -129 should not be taken seriously. Therefore, it is not surprising that those "predic-

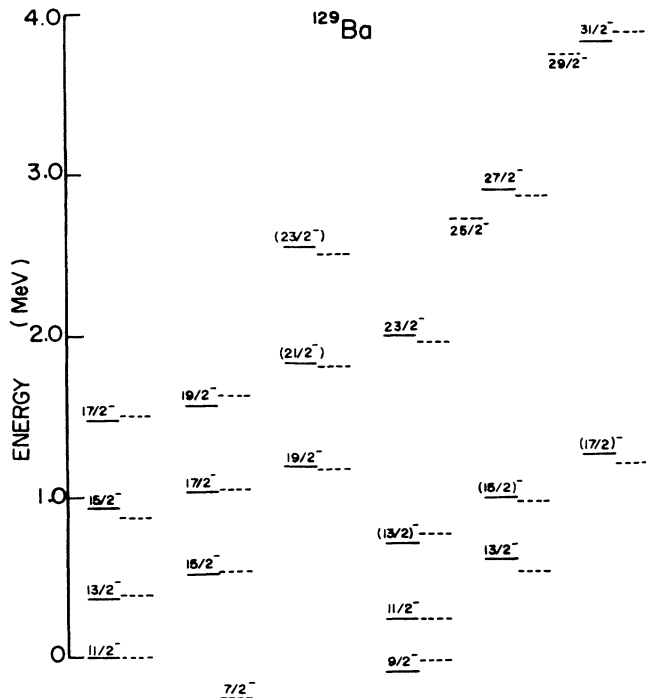


FIG. 7. The experimental and the calculated energy spectra for  $^{129}\text{Ba}$ . The data are taken from Ref. 18.

tions" do not necessarily agree with results from Ref. 1. Incidentally, judging from these three isotopes, the overall agreement between the experimental and the calculated spectra is comparable for the two studies and better in our case for angular momenta  $\frac{19}{2}$ ,  $\frac{21}{2}$ , and  $\frac{23}{2}$  states.

The barium spectra are shown in Figs. 5–7. Comparison with Ref. 1 is restricted to mass numbers 129, 131, and 133. Both works reproduced the most complex  $^{129}\text{Ba}$  spectra with great accuracy. The  $\frac{7}{2}^-$  state is predicted lower than  $\frac{11}{2}^-$ , and a  $\frac{25}{2}^-$  state around 2.7 MeV. In Ref. 1, the calculated positions of both the second  $\frac{13}{2}^-$  level for  $^{131}\text{Ba}$  and  $^{133}\text{Ba}$  are above the yrast  $\frac{15}{2}^-$  level, higher than our result. As in the xenon case, the highest spin states for  $^{131}\text{Ba}$  and  $^{133}\text{Ba}$  are calculated too high in Ref. 1. Our results do not have this tendency. Largest deviations occur for the five highest levels above the  $\frac{31}{2}^-$  level in  $^{125}\text{Ba}$  (not shown in the figure). When the spin gets so high our simple model is not good enough due to properties of the boson core. As is well known from studies of the even-even nuclei, to accurately describe the high spin states beyond the point where backbending occurs, one boson in the core needs to be broken up into two fermions.<sup>6</sup> This helps in two ways: geometrically one can get higher spin values; physically, the fermion interaction is actually responsible for the intricate, noncollective high energy spectra. Hence, in order to describe those high spin states we should include a boson core plus three quasiparticle configurations.<sup>2</sup> For example, if the back-

bending of a certain core nuclide appears at  $I_B = 10$ , then without breaking up the core, our model is good for the neighboring odd-mass nucleus up to angular momentum:  $8 + \frac{11}{2} = \frac{27}{2}$ . Above that, the three quasiparticle configuration is important.

The intensities of the resulting wave functions corresponding to various energy states are analyzed. Naturally, the  $\frac{7}{2}^-$ ,  $\frac{9}{2}^-$ , and  $\frac{11}{2}^-$  states are dominated by the configuration that the fermion moves in  $f_{7/2}$ ,  $h_{9/2}$ , and  $h_{11/2}$  orbits, respectively. For other yrast states,  $h_{11/2}$  is always dominant. Nonyrast levels are usually dominated by another orbit, or not dominated by any one orbit. As examples, the detailed intensity information for  $^{123}\text{Xe}$  and  $^{123}\text{Ba}$  are listed in Table III.

Without reliable experimental information on the electromagnetic transitions to make comparisons, we cannot say too much more. But in the course of the work we believe that a simple boson plus fermion description of the negative-parity states for the odd xenon and barium isotopes is provided by the same model used for the positive-parity states of the corresponding isotopes.<sup>5</sup> In Ref. 5, the wave functions have been tested by a few experimental data. Comparing with Refs. 1 and 2, it is apparent that we have systematically interpreted the isotopic energy spectra with a relatively simple model.

This work was supported by the National Science Council of the Republic of China.

\*Present address: Department of Physics, State University of New York at Stony Brook, Stony Brook, NY 11794-3800.

<sup>1</sup>M. A. Cunningham, Nucl. Phys. **A385**, 204 (1982).

<sup>2</sup>J. M. Arias and C. E. Alonso, Nucl. Phys. **A445**, 333 (1985).

<sup>3</sup>F. Iachello and I. Talmi, Rev. Mod. Phys. **59**, 339 (1987).

<sup>4</sup>R. Bijker and A. E. L. Dieperink, Nucl. Phys. **A379**, 221 (1982).

<sup>5</sup>H. C. Chiang, S. T. Hsieh, and D. S. Chuu, Phys. Rev. C **39**, 2390 (1989).

<sup>6</sup>N. Yoshida, A. Arima, and T. Otsuka, Phys. Lett. **114B**, 86 (1982).

<sup>7</sup>T. Tamura, K. Miyano, and S. Ohya, Nucl. Data Sheets **51**, 329 (1987).

<sup>8</sup>J. Blachot and G. Margreier, Nucl. Data Sheets **50**, 63 (1987).

<sup>9</sup>V. Barci, J. Gizon, A. Gizon, J. Crawford, J. Genevey, A. Plochocki, and M. A. Cunningham, Nucl. Phys. **A383**, 309 (1982).

<sup>10</sup>A. Luukko, J. Hattula, H. Helppi, O. Knuuttila, and F.

Donau, Nucl. Phys. **A357**, 319 (1981).

<sup>11</sup>H. Helppi, J. Hattula, and A. Luukko, Nucl. Phys. **A332**, 183 (1979).

<sup>12</sup>H. Helppi, J. Hattula, A. Luukko, M. Jaaskelainen, and F. Donau, Nucl. Phys. **A357**, 333 (1981).

<sup>13</sup>R. L. Auble, H. R. Hiddleston, and C. P. Browne, Nucl. Data Sheets **17**, 573 (1976).

<sup>14</sup>N. Yoshikawa, J. Gizon, and A. Gizon, J. Phys. (Paris) **40**, 209 (1979).

<sup>15</sup>J. Gizon and A. Gizon, Z. Phys. A **285**, 259 (1978).

<sup>16</sup>J. P. Martin, V. Barci, H. El-Samman, A. Gizon, J. Gizon, W. Klamra, and B. M. Nyako, Nucl. Phys. **A489**, 169 (1988).

<sup>17</sup>J. Gizon and A. Gizon, Z. Phys. A **281**, 99 (1977).

<sup>18</sup>J. Gizon, A. Gizon, and J. Meyer-Ter-Vehn, Nucl. Phys. **A277**, 464 (1977).

<sup>19</sup>Yu V. Sergeenkov and V. M. Sigalov, Nucl. Data Sheets **49**, 639 (1986).